JVI Journals.ASM.org

# Antibody-Dependent Cellular Cytotoxicity-Mediating Antibodies from an HIV-1 Vaccine Efficacy Trial Target Multiple Epitopes and Preferentially Use the VH1 Gene Family

**Mattia Bonsignori,[a] Justin Pollara,[a] M. Anthony Moody,[a] Michael D. Alpert,[b] Xi Chen,[a] Kwan-Ki Hwang,[a] Peter B. Gilbert,[c] Ying Huang,[c] Thaddeus C. Gurley,[a] Daniel M. Kozink,[a] Dawn J. Marshall,[a] John F. Whitesides,[a] Chun-Yen Tsao,[a] Jaranit Kaewkungwal,[d] Sorachai Nitayaphan,[e] Punnee Pitisuttithum,[f] Supachai Rerks-Ngarm,[g] Jerome H. Kim,[h] Nelson L. Michael,[h] Georgia D. Tomaras,[a] David C. Montefiori,[a] George K. Lewis,[i] Anthony DeVico,[i] David T. Evans,[b] Guido Ferrari,[a] Hua-Xin Liao,[a] and Barton F. Haynes[a]**

Duke University Medical Center, Durham, North Carolina, USA[a]; Harvard Medical School, Boston, Massachusetts, USA[b]; Statistical Center for HIV/AIDS Research and Prevention, Fred Hutchinson Cancer Research Center, Seattle, Washington, USA[c]; Tropical Hygiene, Mahidol University, Bangkok, Thailand[d]; Armed Forces Research Institute of Medical Sciences (AFRIMS), Bangkok, Thailand[e]; Clinical Tropical Medicine, Mahidol University, Bangkok, Thailand[f]; Department of Disease Control, Ministry of Public Health, Nonthaburi, Thailand[g]; U.S. Military HIV Research Program, Rockville, Maryland, USA[h]; and Institute of Human Virology, University of Maryland School of Medicine, Baltimore, Maryland[i]

**The ALVAC-HIV/AIDSVAX-B/E RV144 vaccine trial showed an estimated efficacy of 31%. RV144 secondary immune correlate analysis demonstrated that the combination of low plasma anti-HIV-1 Env IgA antibodies and high levels of antibody-dependent cellular cytotoxicity (ADCC) inversely correlate with infection risk. One hypothesis is that the observed protection in RV144 is partially due to ADCC-mediating antibodies. We found that the majority (73 to 90%) of a representative group of vaccinees displayed plasma ADCC activity, usually (96.2%) blocked by competition with the C1 region-specific A32 Fab fragment. Using memory B-cell cultures and antigen-specific B-cell sorting, we isolated 23 ADCC-mediating nonclonally related antibodies from 6 vaccine recipients. These antibodies targeted A32-blockable conformational epitopes ($n = 19$), a non-A32-blockable conformational epitope ($n = 1$), and the gp120 Env variable loops ($n = 3$). Fourteen antibodies mediated cross-clade target cell killing. ADCC-mediating antibodies displayed modest levels of V-heavy (VH) chain somatic mutation (0.5 to 1.5%) and also displayed a disproportionate usage of VH1 family genes (74%), a phenomenon recently described for CD4-binding site broadly neutralizing antibodies (bNAbs). Maximal ADCC activity of VH1 antibodies correlated with mutation frequency. The polyclonality and low mutation frequency of these VH1 antibodies reveal fundamental differences in the regulation and maturation of these ADCC-mediating responses compared to VH1 bNAbs.**

The RV144 ALVAC-HIV (vCP1521) prime/AIDSVAX B/E boost clinical trial provided the first evidence of vaccine-induced protection from acquisition of human immunodeficiency virus type 1 (HIV-1) infection (39). Analysis of immune correlates of risk of infection demonstrated that antibodies (Ab) targeting the Env gp120 V1/V2 region inversely correlated with infection risk, while IgA Env-binding antibodies to Env directly correlated with infection risk (17). In addition, in secondary immune correlate analyses, low plasma IgA Env antibody levels in association with high levels of antibody-dependent cellular cytotoxicity (ADCC) were inversely correlated with infection risk (17). Thus, one hypothesis is that the observed protection in RV144 is due, in a subset of vaccinees, to ADCC-mediating antibodies.

The importance of ADCC responses has been reported in chronically HIV-1-infected individuals (3, 13, 22) and in HIV-1 vaccine studies in nonhuman primates (14, 15, 18, 45). Baum et al. reported an inverse correlation between titers of HIV-1 gp120-specific ADCC antibodies and the rate of disease progression in humans (3). Moreover, HIV-1-infected elite controllers who had undetectable viremia showed higher ADCC antibody titers than infected individuals with viremia (22). In nonhuman primates, administration of vaccine candidates elicited ADCC antibody titers that correlated with control of virus replication after mucosal challenge with a pathogenic simian immunodeficiency virus (SIV) (2, 15). More recently, different groups have reported that titers of nonneutralizing ADCC antibodies are associated with control of viremia against primary SIV infection (14, 18, 45). While antibodies against multiple epitopes can mediate ADCC, it has been recently reported that the A32 monoclonal antibody (MAb), recognizing a conformational epitope in the C1 region of HIV-1 Env gp120 (53), could mediate potent ADCC activity and could block a significant proportion of ADCC-mediating Ab activity detectable in HIV-1-infected individuals (13).

We have recently observed that ADCC-mediating Ab responses are detectable as early as 48 days after acute HIV-1 infection (37). This early appearance of ADCC-mediating Abs after acute HIV-1 infection contrasts with HIV-1 broadly neutralizing antibodies (bNAbs) that appear approximately 2 to 4 years after HIV-1 infection (16, 27, 42).

In this study, we have defined a series of modestly somatically mutated ADCC-mediating antibodies induced by the ALVAC-HIV/AIDSVAX B/E vaccine (34, 39), most of which are directed against conformational A32-blockable epitopes of the gp120 en-

**Received** 24 April 2012 **Accepted** 24 July 2012
**Published ahead of print** 15 August 2012
Address correspondence to Mattia Bonsignori, mattia.bonsignori@duke.edu.
M.B., J.P., M.A.M., G.F., H.-X.L., and B.F.H. contributed equally to this work.

doi:10.1128/JVI.01023-12

velope glycoprotein. This group of antibodies displayed preferential use of the variable heavy 1 (VH1) gene segment, a phenomenon similar to that recently described for highly mutated CD4 binding-site (CD4bs)-specific bNAbs (41, 52).

## MATERIALS AND METHODS

**Plasma and cellular samples from vaccine recipients.** All trial participants gave written informed consent as described for both studies (34, 39). Samples were collected and tested according to protocols approved by the institutional review boards at each site involved in these studies. Plasma samples were obtained from volunteers enrolled in the phase I/II clinical trial (34) and in the community-based, randomized, multicenter, double-blind, placebo-controlled phase III efficacy trial (39); both trials tested the prime-boost combination of vaccines containing ALVAC-HIV (vCP1521) (Sanofi Pasteur) and AIDSVAX B/E (Global Solutions for Infectious Diseases). Plasma samples collected at enrollment (week 0) and 2 weeks after the last immunization (week 26) were selected by simple random sampling with a vaccine/placebo ratio of 40:10 for both men and women.

Peripheral blood mononuclear cells (PBMCs) from six vaccine recipients enrolled in the phase II ($n = 3$) and phase III ($n = 3$) trials whose plasma showed ADCC activity were used for isolation of memory B cells and monoclonal antibodies (MAbs). Subjects T141485, T141449, and T143859 participated in the phase II trial; subjects 609107, 210884, and 347759 were enrolled in the phase III trial. All six subjects had negative serology for HIV-1 infection at the time of collection.

**Competition binding assay.** To determine the presence of A32 binding Ab in the plasma of the vaccine recipients, we modified the previously described full-length single-chain (FLSC) assay (9). Briefly, biotinylated A32 was used at a limiting dilution of 0.173 μg/ml to compete for the binding of plasma Ab to a single-chain complex (FLSC) captured (Aby D7324) on a plate. Plasma samples from 80 vaccine recipients and 20 placebo recipients were initially screened at a 1:50 final dilution. For plasma samples that blocked binding of biotinylated A32 MAb, the ability to mediate ≥50% of A32 blocking at 1:50 dilution was used as the criterion for inclusion in this study. Seventy-nine plasma samples met this criterion (data not shown) and were tested in a serial dilution to calculate the 50% inhibitory dose ($ID_{50}$) titer.

**ADCC-luciferase (ADCC-92TH023) assay.** Plasma was evaluated for ADCC activity against cells infected by HIV-1 92TH023 in an assay that employs a natural killer (NK) cell line as effectors. The NK cell line was derived from KHYG-1 cells (Japan Health Sciences Foundation) (54). These cells were transduced with a retroviral vector to stably express the V158 variant of human CD16a (FCGR3A). The target cells were CEM.$NKR_{CCR5}$ cells (AIDS Research and Reference Reagent Program, Division of AIDS, NIAID, NIH; contributed by Alexandra Trkola) (47), which were modified to express Firefly luciferase upon infection. Target cells were infected with HIV-1 92TH023 by spinoculation (35) 4 days prior to use in assays. NK effectors and 92TH023-infected targets were incubated at an effector/target (E/T) ratio of 10:1 in the presence of triplicate serial dilutions of plasma samples for 8 h. Wells containing NK cells and uninfected targets without plasma defined 0% relative light units (RLU), and wells with NK cells plus infected targets without plasma defined 100% RLU. ADCC activity was measured as the percent loss of luciferase activity with NK cells plus infected targets in the presence of plasma.

**Recombinant gp120 HIV-1 proteins.** Where indicated, CEM.$NKR_{CCR5}$ target cells were coated with recombinant gp120 HIV-1 protein from the CM243 isolate representing the subtype A/E HIV-1 envelope (GenBank accession no. AY214109; Protein Sciences, Meiden, CT). The optimum amount to coat target cells was determined as previously described (36).

**Virus and IMCs for ADCC GTL assay.** HIV-1 reporter viruses used were replication-competent infectious molecular clones (IMC) designed to encode subtype A/E, B, or C *env* genes in *cis* within an isogenic backbone that also expresses the Renilla luciferase reporter gene and preserves all viral open reading frames (10). The Env-IMC-LucR viruses used were subtype A/E NL-LucR.T2A-AE.CM235-ecto ($IMC_{CM235}$) (GenBank accession no. AF259954.1; plasmid provided by Jerome Kim, U.S. Military HIV Research Program), subtype B NL-LucR.T2A-BaL.ecto ($IMC_{BaL}$) (1), subtype C NL-LucR.T2A-DU422.ecto ($IMC_{DU422}$; GenBank accession no. DQ411854), and subtype C NL-LucR.T2A-DU151.ecto ($IMC_{DU151}$; GenBank accession no. DQ411851). Reporter virus stocks were generated by transfection of 293T cells with proviral IMC plasmid DNA and titrated on TZM-bl cells for quality control.

**ADCC-GTL assay.** ADCC activity was detected according to our previously described ADCC-GranToxiLux (GTL) procedure (36). We used the following target cells: CM243 gp120 coated (ADCC-CM243 assay) and $IMC_{CM235}$-, $IMC_{BaL}$-, $IMC_{DU422}$-, and $IMC_{DU151}$-infected CEM.$NKR_{CCR5}$ cells (ADCC-E.CM235, ADCC-B.BaL, ADCC-C.DU422, and ADCC-C.DU151 assay, respectively) (47). All of the PBMC samples from the seronegative donors used as effector cells were obtained according to the appropriate institutional review board protocol. We used 10,000 target cells per well, and E/T ratios of 30:1 and 10:1 were used for whole PBMC and purified NK effector cells, respectively. MAb A32 (James Robinson, Tulane University, New Orleans, LA), palivizumab (MedImmune, LLC, Gaithersburg, MD; used as a negative control), and vaccine-induced MAbs were tested as six 4-fold serial dilutions starting at a concentration of 40 μg/ml (range, 40 to 0.039 μg/ml). For the Fab blocking assay, the target cells were incubated for 15 min at room temperature in the presence of 10 μg/ml A32, 19B (31), and 17B (46) Fab fragments, which were produced by Barton Haynes. The excess Fab was removed by washing the target cell suspensions once before plating with the effector cells as previously described (13). A minimum of $2.5 \times 10^3$ events representing viable gp120-coated or infected target cells was acquired for each well. Data analysis was performed using FlowJo 9.3.2 software. The results are expressed as percent granzyme B (GzB) activity, defined as the percentage of cells positive for proteolytically active GzB out of the total viable target cell population. The final results are expressed after subtracting the background represented by the percent GzB activity observed in wells containing effector and target cell populations in the absence of MAb, IgG preparation, or plasma. The results were considered positive if the percent GzB activity after background subtraction was >8% for the gp120-coated cells or >5% for the CM235-infected target cells.

**Isolation of ADCC-mediating monoclonal antibodies.** Monoclonal antibodies were isolated either from $IgG^+$ memory B cells cultured at nearly clonal dilution for 14 days (4), followed by sequential screenings of culture supernatants for HIV-1 gp120 Env binding and ADCC activity, or from memory B cells that bound to the HIV-1 group M consensus $gp140_{Con.S}$ Env sorted by flow cytometry (16).

Subject 210884 was tested using $IgG^+$ memory B-cell cultures isolated and cultured at nearly clonal dilutions as previously described (4). Briefly, 57,600 $IgG^+$ memory B cells were isolated from frozen PBMCs by selecting $CD2^-$, $CD14^-$, $CD16^-$, $CD235a^-$, $IgD^-$, and $IgG^+$ cells through two rounds of separation with magnetic beads (Miltenyi Biotec, Auburn, CA) and resuspended in complete medium containing 2.5 μg/ml oCpG ODN2006 (tlrl-2006; InvivoGen, San Diego, CA), 5 μM CHK2 kinase inhibitor (Calbiochem/EMD Chemicals, Gibbstown, NJ), and Epstein-Barr virus (EBV; 200 μl supernatant of B95-8 cells/$10^4$ memory B cells). After overnight incubation in bulk, cells were distributed into 96-well round-bottom tissue culture plates at a cell density of 8 cells/well in the presence of ODN2006, CHK2 kinase inhibitor, and irradiated (7,500 cGy) CD40 ligand-expressing L cells (5,000 cells/well). Cells were refed at day 7 and harvested at day 14.

Subjects T141485, T141449, T143859, and 609107 were tested using antigen-specific memory B-cell sorting as previously described (16), with the following modifications. The group M consensus $gp140_{Con.S}$ Env labeled with Pacific Blue and Alexa fluor 647 (Invitrogen, Carlsbad, CA) was used for sorting. Memory B cells were gated as Aqua vital $dye^-$, $CD3^-$, $CD14^-$, $CD16^-$, $CD235a^-$, $CD19^+$, and surface $IgD^-$; memory B cells

stained with $gp140_{Con.S}$ in both colors were sorted as single cells as described previously (16). A total of 137,345 memory B cells were screened using this method: 32,766 from subject T141485, 54,621 from subject T141449, 20,629 from subject T143859, and 29,329 from subject 609107.

For subject 347759, memory B cells were screened using both methods: 57,600 cells were cultured at nearly clonal dilution and 69,400 memory B cells were sorted. Sorted cells were previously enriched for $IgG^+$ memory B cells as described above, incubated overnight in complete medium containing 2.5 μg/ml oCpG ODN2006, 5 μM CHK2 kinase inhibitor, and EBV (200 μl supernatant of B95-8 cells/$10^4$ memory B cells), and then stimulated for 7 days at a cell density of 1,000 cells/well in the presence of ODN2006, CHK2 kinase inhibitor, and irradiated CD40 ligand-expressing L cells (5,000 cells/well).

**Isolation of V(D)J immunoglobulin regions.** Single-cell PCR was performed as previously described (25, 50). Briefly, reverse transcription (RT) was performed using Superscript III reverse transcriptase (Invitrogen, Carlsbad, CA) and human constant region primers for IgG, $IgA_1$, $IgA_2$, IgM, IgD, Igκ, and Igλ; separate reactions amplified individual $V_H$, $V_κ$, and $V_λ$ families from the cDNA template using two rounds of PCR. Products were analyzed with agarose gels (1.2%) and purified with PCR purification kits (Qiagen, Valencia, CA). Products were sequenced in forward and reverse directions using a BigDye sequencing kit using an ABI 3700 device (Applied Biosystems, Foster City, CA). Sequence base calling was performed using Phred (11, 12); forward and reverse strands were assembled using an assembly algorithm based on the quality scores at each position (32). The estimated PCR artifact rate was 0.28 or approximately one PCR artifact per five genes amplified. Ig isotype was determined by local alignment with genes of known isotype (44); V, D, and J region genes, CDR3 loop lengths, and mutation rates were identified using SoDA (48), and data were annotated so that matching subject data and sort information were linked to the cDNA sequence and analysis results.

**Expression of recombinant antibodies.** Isolated Ig V(D)J gene pairs were assembled by PCR into linear full-length Ig heavy- and light-chain gene expression cassettes (25) and optimized as previously described for binding to the Fcγ receptors (43). Human embryonic kidney cell line 293T (ATCC, Manassas, VA) was grown to near confluence in 6-well tissue culture plates (Becton Dickson, Franklin Lakes, NJ) and transfected with 2 μg per well of purified PCR-produced IgH and IgL linear Ig gene expression cassettes using Effectene (Qiagen). The supernatants were harvested from the transfected 293T cells after 3 days of incubation at 37°C in 5% $CO_2$, and the monoclonal antibodies were purified as previously described (25).

**Direct binding ELISAs.** Three hundred eighty-four-well plates (Corning Life Sciences, Lowell, MA) were coated overnight at 4°C with 15 μl of purified HIV-1 monomeric gp120 envelope glycoprotein (E.A244 gp120, B.MN gp120, and A.92TH023 gp120) antigen at 2 μg/ml and blocked with assay diluent (phosphate-buffered saline [PBS] containing 4% [wt/vol] whey protein–15% normal goat serum–0.5% Tween 20–0.05% sodium azide) for 1 h at room temperature.

Ten μl/well of purified MAbs was incubated for 2 h at room temperature in serial 3-fold dilutions starting at 100 μg/ml for the determination of 50% effective concentrations ($EC_{50}$) and then washed with PBS–0.1% Tween 20. Thirty μl/well of alkaline phosphatase-conjugated goat anti-human IgG in assay diluent was added for 1 h, washed, and detected with 30 μl/well of *p*-nitrophenyl phosphate substrate diluted in 50 mM $NaHCO_3$ plus $Na_2CO_3$ (1:1, vol/vol), pH 9.6, 10 mM $MgCl_2$. Plates were developed for 45 min in the dark at room temperature and read at an optical density of 405 nm ($OD_{405}$) with a VersaMax microplate reader (Molecular Devices, Sunnyvale, CA).

Epitope mapping studies were performed using 15-mer linear peptides spanning the gp120 envelope glycoprotein of the MN and 92TH023 HIV-1 strains obtained from the AIDS Reagent Repository as coating antigens, horseradish peroxidase goat anti-human IgG as secondary antibody, and 3,3′,5,5′-tetramethylbenzidine (TMB) substrate for detection.

**TABLE 1** Frequency of ADCC responders among vaccine and placebo recipients before and after vaccination

| Recipient group (*n*) and time point | Assay result (no. of responders [%, 95% CI]) | |
|---|---|---|
| | ADCC-CM243 | ADCC-92TH023 |
| Vaccine (40) | | |
| Wk 0 | 0 (0, 0–31) | 4 (10, 2.8–23.7) |
| Wk 26 | 36 (90, 76–97) | 29 (72.5, 56.1–85.4) |
| Placebo (10) | | |
| Wk 0 | 1 (10, 0–44.5) | 0 (0, 0–31) |
| Wk 26 | 1 (10, 0–44.5) | 1 (10, 0.3–44.5) |

**Statistical analyses.** The analysis of the ADCC-mediating Ab responses in the plasma of the vaccine recipients was conducted as follows. For each time point of a subject, partial area under the activity versus the log10 (dilution) curve (AUC) was estimated nonparametrically for each assay. For ADCC-CM243 assay using gp120-coated target cells, the AUC was calculated based on percent GzB activity across dilution levels of 50, 250, 1,250, 6,250, 31,250, and 156,250; for ADCC-92TH023 assay using infected cells, the AUC was calculated based on percent loss of luciferase activity across dilution levels of 32, 100, 316, and 1,000. Two-sample *t* test allowing for unequal variance was used to test the mean difference in AUC between the vaccine and placebo groups at week 26. A paired *t* test was used to test the mean difference in AUC between week 26 and week 0 among vaccinees. For each of the vaccine and placebo groups and for each time point, the positive response rate was estimated by the observed fraction of subjects that have a positive response (defined as peak percent GzB greater than 8% for the ADCC-CM243 assay and peak percent loss of luciferase activity greater than 9% for the ADCC-92TH023 assay). A 95% confidence interval (CI; computed by the Agresti-Coull method) was provided around each response rate. An exact *P* value from McNemar's test was used to evaluate whether the response rate differs for the week 26 time point versus the week 0 time point among vaccinees. Fisher's exact test was used to provide a *P* value to test whether the response rate differed between the vaccine and placebo groups at week 26.

The other statistical analyses conducted in this study were performed using Prism software v5.0c (GraphPad Software, Inc.), and the appropriate methods are listed throughout the manuscript.

## RESULTS

**Vaccine-induced ADCC responses.** We studied 50 simple randomly sampled plasma specimens drawn from subjects enrolled in the RV144 vaccine trial at enrollment (week 0) and 2 weeks after the last immunization (week 26), including 10 placebo recipients (5 male and 5 female) and 40 vaccine recipients (20 male and 20 female; four injections of recombinant canarypox vector vaccine ALVAC-HIV [vCP1521] and two booster injections of recombinant gp120 subunit [AIDSVAX B/E]) (34, 39). The frequency of ADCC responders (Table 1) and the AUC for ADCC activity (Fig. 1A to D) of both vaccine and placebo recipients were measured using two ADCC assays, $CEM.NKR_{CCR5}$ target cells either coated with HIV-1 AE.CM243 gp120 (ADCC-CM243) (36) or infected with the AE.92TH023 HIV-1 strain (ADCC-92TH023) (17).

The ADCC response rate measured with the ADCC-CM243 assay increased from 0% at week 0 to 90% at week 26 among the vaccine recipients (Table 1). Similarly, the ADCC-92TH023 assay detected activity in 72.5% (29/40) of vaccine recipients at week 26 (Table 1). For both assays, the frequency of positive responses among the vaccine recipients was significantly higher comparing baseline (week 0) to postimmunization (week 26) ($P < 0.0001$ for both assays).

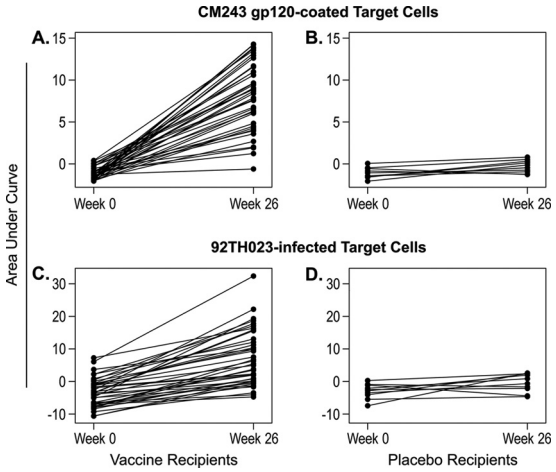


**FIG 1** Vaccine-induced ADCC responses. To measure plasma ADCC activity induced by the ALVAC-HIV(vCP1521)/AIDSVAX B/E vaccine, plasma samples from 40 vaccine recipients and 10 placebo recipients were collected before immunization (week 0) and 2 weeks after the last boost (week 26). ADCC activity was measured using the ADCC-CM243 assay (A and B) and ADCC-92TH023 assay (C and D) as described in Materials and Methods. Results are reported as areas under the curve (AUC). Each dot represents one sample. The lines connect samples obtained from the same donor.

We next evaluated the AUC of a dilution of antibody in the assay (see the statistical analysis in Materials and Methods). In both the ADCC-CM243 and ADCC-92TH023 assays, AUC values of vaccinated subjects at week 26 were significantly higher than both of those in the vaccine recipients at week 0 and in the placebo group at week 26 ($P < 0.0001$ and $P < 0.001$, respectively) (Fig. 1A to D). Thus, the ALVAC-HIV/AIDSVAX B/E vaccine induced anti-HIV-1 gp120 ADCC activity in ~70 to 90% of vaccine recipients depending on the assay utilized. This frequency of responders among vaccinees is similar to that reported in earlier phase II studies as well as in RV144 (17, 21). It is important to note that the 92TH023-infected target cell ADCC assay was used in the RV144 immune correlate primary analysis, and in the secondary analysis, high activity in this assay associated with low plasma anti-Env IgA responses inversely correlated with infection risk (17).

**Plasma ADCC activity is blocked in part by MAb A32.** Since MAb A32 can block plasma ADCC responses during chronic infection (13), we sought to determine whether A32-like antibodies were produced by RV144 vaccine recipients. We first evaluated the ability of plasma samples collected at week 26 postvaccination from simple random samples drawn from both RV144 vaccine ($n$ = 79 out of 80; one sample was not studied because of less than 50% inhibition at screening) and placebo ($n$ = 20) recipients for their ability to block the binding of biotinylated A32 MAb to B.BaL Env. Plasma Ab blocked A32 MAb binding in 76/79 (96.2%) of the vaccine recipients with an average 50% inhibitory dose ($ID_{50}$) titer of 119 (95% CI, 95 to 130) (Fig. 2A). These data demonstrated the presence of A32-like antibodies in the plasma of vaccine recipients.

We then evaluated the effect of pretreatment of CM243 gp120-coated target cells with A32 Fab on plasma-mediated ADCC (13). Thirty vaccine recipients whose plasma samples were previously identified to mediate ADCC were selected to represent each tertile (low, medium, and high response) of the range of ADCC activities observed. These plasma samples were tested to determine the dilution that provided maximum ADCC activity (data not shown). When tested at the optimal dilution, these plasma samples induced granzyme B (GzB) activity against AE.CM243 gp120-coated target cells ranging from 8.0 to 34.6% (mean ± standard deviation [SD], 20.4 ± 6.6) (Fig. 2B). When the cells were pretreated with 10 μg/ml of A32 Fab, ADCC activity was reduced or completely abrogated for each plasma sample (GzB activity, ≤3.2%; $P < 0.001$ versus untreated samples) (Fig. 2B). Similar treatment with a control Fab made from palivizumab (19) did not affect plasma ADCC activity (range, 9.0 to 35.8%; mean ± SD, 21.1% ± 6.7%) (Fig. 2B). However, preincubation with 10 and 50 μg/ml of A32 Fab did not block plasma ADCC activity at the peak of responses (1:50 dilution) in ADCC assays using target cells infected with either the E.92TH023 or the E.CM235 HIV-1 strains (data not shown). This lack of inhibition may be due to unfavorable kinetics for Fab epitope recognition on infected cells in the

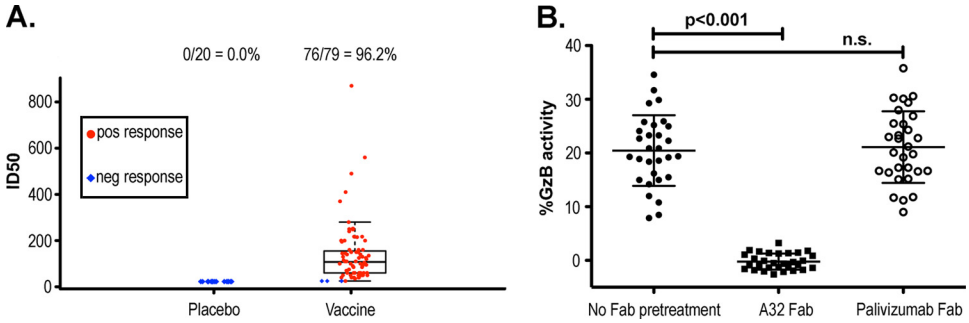


**FIG 2** Recognition of the A32 epitope in plasma of ALVAC-HIV(vCP1521)/AIDSVAX B/E vaccine recipients. (A) Plasma samples collected at week 26 from 20 placebo recipients and 79 vaccine recipients were evaluated for the presence of Abs with A32-like binding specificities by competition ELISA. We defined plasma samples that inhibited >50% of A32 MAb binding as positive (red dots). While none of the placebo recipients displayed A32-like responses, the plasma of 76/79 vaccine recipients (96.2%) competed for A32 MAb binding to its cognate epitope. The whisker boxes show the average plasma $ID_{50}$ titer and the 95% confidence intervals for each test group. (B) Inhibition of plasma ADCC activity by epitope blocking with the MAb A32 Fab fragment was evaluated in the ADCC-CM243 assay (see Materials and Methods). Plasma samples were collected at week 26 from 30 vaccine recipients and were tested at dilutions corresponding to peak activity. Data are reported as maximum percent GzB activity detected using CM243-gp120-coated targets without pretreatment (no Fab pretreatment; left) or treated with 10 μg/ml MAb A32 Fab (center) or palivizumab Fab (negative control; right). Lines and error bars represent the mean percent GzB activity ± SD. The $P$ values were obtained using repeated-measure analysis of variance. pos, positive; neg, negative; n.s., not significant.

presence of polyclonal antibodies in plasma. To better define the nature of the antibodies responsible for the observed ADCC activity, we isolated ADCC-mediating MAbs from ALVAC-HIV/AIDSVAX B/E vaccine recipients.

**Isolation of ADCC-mediating antibodies from ALVAC-HIV/AIDSVAX B/E vaccinees.** We isolated a total of 23 MAbs that mediated ADCC from memory B cells of six vaccine recipients enrolled in the RV135 phase II ($n = 3$) (21, 34) or RV144 phase III ($n = 3$) (39) ALVAC-HIV/AIDSVAX B/E clinical trials. Nine MAbs (CH49, CH51, CH52, CH53, CH54, CH55, CH57, CH58, and CH59) were obtained from cultured $IgG^+$ memory B cells that bound to one or more of the E.A244, B.MN, and E.92TH023 gp120 envelope glycoproteins, while the remaining 14 were obtained from group M consensus $gp140_{Con.S}$ Env-specific flow-cytometric single-memory-B-cell sorting (4, 16). Two of the 23 ADCC-mediating MAbs were against the gp120 Env V2 region and are the subject of a separate report (H.-X. Liao, M. Bonsignori, B. F. Haynes, unpublished data).

ADCC activity of the remaining 21 MAbs, purified and expressed in a codon-optimized IgG1 backbone, was measured using both E.CM243 gp120-coated (ADCC-CM243) and E.CM235-infected (ADCC-CM235) target cells in the flow-based assay described in Materials and Methods. The maximum percent GzB activity of the 21 MAbs ranged from 38.9% (CH54) to 6.0% (CH92) (Fig. 3A). Remarkably, 11/21 MAbs displayed a maximum percent GzB activity greater than that of A32 MAb (16%) in duplicate assays: CH54 (38.9%), CH55 (31.4%), CH57 (31.3%), CH23 (31.2%), CH49 (26.7%), CH51 (25.9%), CH53 (24.4%), CH52 (23.9%), CH40 (22.6%), and CH20 (21.0%). The endpoint titers of each of the 21 MAbs (Fig. 3B) ranged from <20 ng/ml to 30.3 μg/ml (means ± SD, 4.1 ± 8.8 μg/ml).

None of the ADCC-mediating MAbs were heavily somatically mutated: the mean nucleotide mutation frequencies of the heavy and light chains were 2.4% (range, 0.5 to 5.1%) and 1.8% (range, 0.4 to 4.3%), respectively (Table 2). These data demonstrate that the ALVAC-HIV/AIDSVAX B/E vaccine induced polyclonal antibody responses capable of mediating moderate to high levels of ADCC activity without requiring high levels of ADCC antibody affinity maturation.

**Epitope mapping of vaccine-induced ADCC-mediating antibodies.** To define the specificity of ADCC-mediating MAbs, we asked if they recognized linear epitopes by testing their ability to bind to overlapping linear peptides spanning the gp120 envelope glycoprotein of the B.MN or E.92TH023 HIV-1 strain. Each MAb bound to one or more of the vaccine gp120 envelope glycoproteins, which included the B.MN and E.92TH023 strains (Table 3). We found that 19/20 MAbs (CH53 was not tested) did not react with any of the B.MN or E.92TH023 peptides, while one (CH23) reacted with the clade E V3 loop (NTRTSINIGRGQVFY). As previously described, we used the A32 Fab blocking strategy in the ADCC-CM235 assay to determine whether the ADCC activity of the 20 MAbs not specific for the V3 loop was mediated by targeting conformational epitopes expressed on infected cells that could be blocked by the A32 MAb (Fig. 4). As a control, we also tested the ability of these 20 MAbs to block the ADCC activity mediated by 17B and 19B Fab fragments, which target the CD4-induced (CD4i) and V3 epitopes, respectively (Fig. 4). In contrast to plasma ADCC activity, which could not be blocked by A32 when tested against CM235-infected target cells, A32 Fab blocking inhibited between 73 and 100% (means ± SD, 92% ± 9%) of the

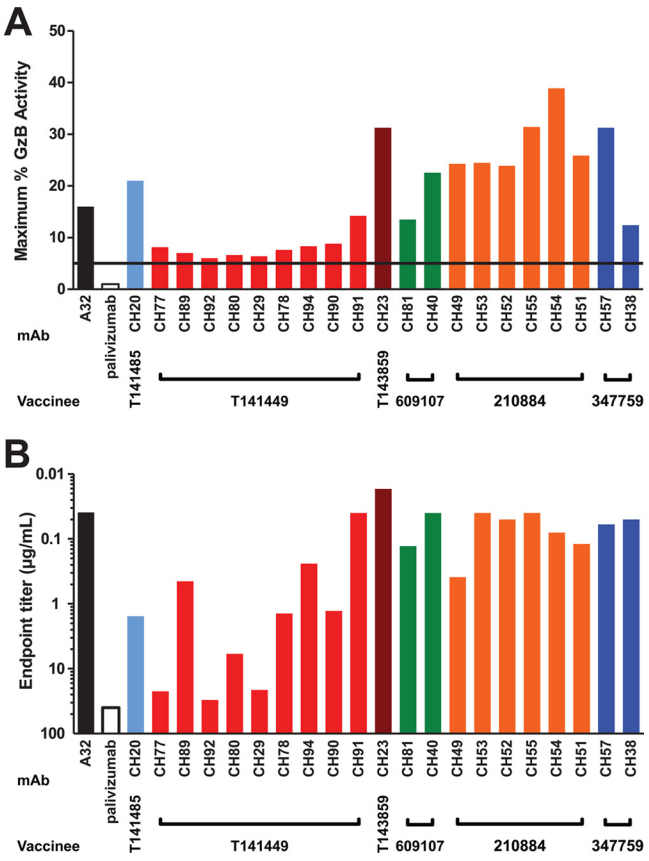


**FIG 3** ADCC activity of vaccine-induced MAbs. ADCC activity mediated by monoclonal antibodies isolated from memory B cells of ALVAC-HIV-(vCP1521)/AIDSVAX B/E vaccine recipients. Twenty-three MAbs were isolated from six vaccine recipients. Each bar is color-coded by subject: T141485 (light blue), T141449 (red), T143859 (brown), 609107 (green), 210884 (orange), and 347759 (dark blue). MAb A32 (positive control) and palivizumab (negative control) are shown in black and white, respectively. (A) The plots show the maximum percent GzB with the threshold of positivity (5%) indicated by the black line. (B) The endpoint titer expressed in μg/ml for each MAb. The threshold of positivity was determined by averaging the results obtained by testing more than 70 MAbs with different binding capacities to gp120 and infected cells. Data shown refer to the results obtained with the ADCC-CM235 assay with the exception of MAb CH23, for which results of the ADCC-CM243 assay are shown. ADCC activity of all MAbs was confirmed in the ADCC-CM235 assay with a 6-h incubation (not shown; $P = 0.001$ by Spearman correlation analysis).

ADCC activity mediated by 19/20 (95%) non-V3 MAbs (Fig. 4). CH20 was not inhibited by any of the A32, 17B, or 19B Fab fragments (Fig. 4). None of the MAbs displayed substantial loss of ADCC activity (defined as >20% inhibition) when E.CM235-infected target cells were preincubated with Fab fragments of MAb 17B or 19B (Fig. 4).

To confirm the results observed with the ADCC assay, we tested the ability of the ADCC-mediating MAbs to block A32 binding to the AE.A244 gp120 envelope glycoprotein and found that 16 MAbs blocked 20.7 to 94% of A32 binding to gp120 Env (Fig. 5). As expected, MAb CH20 did not block MAb A32 binding to gp120 Env, consistent with the inability of A32 Fab to block CH20-mediated ADCC activity. Of note, CH29 and CH57 did not reciprocally block A32 binding to the envelope, even though A32 Fab blocked their ADCC activity (Fig. 4) and MAb A32 blocked their binding to Env (Table 3).

**TABLE 2** Characteristics of the V(D)J rearrangements of vaccine-induced ADCC-mediating monoclonal antibodies

| | | Characteristics of rearrangement by chain | | | | | | | | | | |
|---|---|---|---|---|---|---|---|---|---|---|---|---|
| | | Heavy | | | | | | Light | | | | |
| PTID[a] | MAb | Isotype | V | D | J | CDR3[b] | Mutation frequency[c] (%) | Type | V | J | CDR3[b] | Mutation frequency[c] (%) |
| T141485 | CH20 | G1 | 1-69*02 | 6-6*01 | 4*02 | 15 | 2.6 | λ | 2-23*02 | 3*02 | 10 | 0.4 |
| T141449 | CH77 | G3 | 1-2*02 | 2-OF15*02 | 6*02 | 15 | 2.3 | κ | 4-1*01 | 4*01 | 8 | 0.8 |
| | CH89 | G3 | 1-2*02 | 3-22*01 | 4*02 | 12 | 2.1 | κ | 1-39-*01 | 4*01 | 9 | 1.4 |
| | CH92 | G1 | 1-2*02 | 2-15*01 | 4*02 | 19 | 1.7 | κ | 1D-12*01 | 5*01 | 9 | 2.6 |
| | CH80 | G1 | 1-2*02 | 1-IR1*01C | 4*02 | 12 | 1.6 | κ | 1-27*01 | 4*01 | 10 | 1.1 |
| | CH29 | A2 | 1-2*02 | 2-15*01 | 4*02 | 12 | 0.8 | κ | 1-39*01 | 1*01 | 9 | 0.6 |
| | CH78 | G1 | 1-2*02 | 3~22*01 | 4*02 | 19 | 0.7 | κ | 3-11*01 | 1*01 | 9 | 1.1 |
| | CH94 | G1 | 1-46*02 | 5-12*01 | 6*02 | 23 | 2.2 | κ | 1-39*01 | 2*01 | 9 | 1.7 |
| | CH90 | G1 | 1-46*01 | 3-10*01 | 4*02 | 14 | 1.5 | κ | 1-13*02 | 1*01 | 9 | 4.3 |
| | CH91 | G1 | 4-31*03 | 4-17*01 | 3*02 | 15 | 2.0 | λ | 2-11*01 | 3*02 | 11 | 1.4 |
| T143859 | CH23 | G1 | 3-66*01 | 3-OR15*3 | 1*01 | 11 | 4.5 | λ | 6-57*01 | 3*02 | 10 | 2.2 |
| 609107 | CH81 | G1 | 1-8*01 | 3-10*01 | 4*02 | 19 | 0.5 | κ | 1-39*01 | 2*01,02 | 9 | 1.4 |
| | CH40 | G1 | 1-46*02 | 6-6*01 | 5*02 | 15 | 3.6 | κ | 3-20*01 | 4*01 | 5 | 0.9 |
| 210884 | CH49 | G1 | 1-2*02 | 1-26*01 | 4*02 | 16 | 5.1 | λ | 2-11*01 | 3*02 | 10 | 3.1 |
| | CH53 | G1 | 1-2*02 | 2-2*01,02 | 4*02 | 16 | 2.3 | λ | 2-11*01 | 2*01 | 10 | 2.4 |
| | CH52 | G1 | 1-2*02 | 6-13*01 | 4*02 | 13 | 1.4 | κ | 3-20*01 | 2*01 | 10 | 1.8 |
| | CH55 | G1 | 1-46*01 | 1-1*01 | 5*02 | 15 | 4.3 | κ | 3-15*01 | 5*01 | 10 | 1.5 |
| | CH54 | G1 | 1-58*02 | 1-26*01 | 5*02 | 14 | 2.1 | κ | 1-39*01 | 2*01 | 9 | 1.4 |
| | CH51 | G1 | 4-34*12 | 3-10*01 | 4*02 | 14 | 0.5 | κ | 3-20*01 | 1*01 | 8 | 0.6 |
| 347759 | CH57 | G1 | 1-2*02 | 1-1*01 | 6*02 | 12 | 3.4 | κ | 1-39*01 | 1*01 | 9 | 4.0 |
| | CH38 | A1 | 3-23*01 | 3-10*01,02 | 1*01 | 12 | 4.7 | λ | 2-14*03 | 3*02 | 10 | 3.6 |

[a] PTID, participant identity.
[b] CDR3, complementarity determining region 3. Length is expressed as amino acids according to the Kabat numbering system (20).
[c] Nucleotide mutation frequency in V gene as determined by SoDA (48).

We found that 6/19 (32%) of the A32-blockable MAbs partially blocked the binding of soluble CD4 (sCD4) and/or MAb b12 to gp120 envelope glycoproteins (Table 3). This activity ranged from 22% (CH77) to 46% (CH40) blocking of sCD4 binding to AE.A244 gp120 Env and from 25% (CH40) to 40% (CH55) blocking of b12 binding to B.JRFL gp120 Env; in some cases blocking was higher than that seen for A32 (Table 3). These data suggest that these ADCC-mediating MAbs interfere with binding of CD4bs-directed MAbs either by inducing conformational changes on the gp120 envelope glycoprotein or by partially blocking access to the CD4bs. The combination of blocking and binding data indicate that the ALVAC-HIV/AIDSVAX B/E vaccine induced a group of antibodies that mediate ADCC by targeting distinct but overlapping Env epitopes that are mostly A32 blockable.

Moreover, it should be noted that the original isotypes of CH29 and CH38 were $IgA_1$ and $IgA_2$, respectively (Table 2). When CH29 and CH38 were expressed as $IgG_1$ MAbs, they mediated ADCC activity (GzB activities of 6.4% [CH29] and 12.4% [CH38]) that was directed against the gp120 C1 region, as demonstrated by blocking with the A32 Fab (Fig. 4).

**Cross-clade ADCC activity of RV144-induced antibodies.** We next studied the ability of the 21 MAbs to mediate ADCC against viruses from different HIV-1 subtypes. MAb A32 mediated ADCC against all four tested isolates with an endpoint titer of 0.039 μg/ml against all strains (Fig. 6). Each of the 21 MAbs derived from vaccinees were able to mediate ADCC against target cells infected with the subtype A/E strain virus AE.CM235, while 14/21 MAbs (67%) mediated ADCC against those infected with B.Bal. When tested against subtype C virus isolates, 4/21 (19%) mediated ADCC against C.DU151-infected target cells while a single recovered MAb (CH54) mediated ADCC against C.DU422-infected target cells (Fig. 6). The patterns of cross-clade ADCC activity, combined with the patterns observed in binding and blocking experiments, demonstrate that the RV144 immunogen elicited a diverse set of antibodies directed at epitopes overlapping, but not identical to, that of MAb A32.

**VH1 gene family members are overrepresented among ADCC-mediating monoclonal antibodies recovered from vaccine recipients.** Association of anti-HIV-1 ADCC activity with the use of a specific VH family gene has not been previously reported. It was therefore quite surprising to find that 17/23 (74%) of ADCC-mediating MAbs isolated from the vaccine recipients utilized the VH1 family gene (Fig. 7); this group includes the two anti-V2 MAbs that are described in a separate report (23), which did not use VH1. In contrast, only 19/111 (17.1%) heavy chains isolated from memory B-cell cultures that did not mediate ADCC used VH1 family gene segments. The frequency of VH1 family gene usage was significantly lower than that for the 23 ADCC-mediating antibodies ($P < 0.0001$ by Fisher's exact test), demonstrating that the high frequency of VH1 gene usage among ADCC-mediating MAbs was not reflective of a disproportionate use of VH1 among recovered antibodies from vaccinees.

**TABLE 3** HIV-1 Env binding of vaccine-induced ADCC-mediating MAbs and blocking of sCD4 and b12 binding to Env

| PTID[a] and MAb | Binding[b] of MAbs to HIV-1 Env | | | % Blocking by MAb | | |
|---|---|---|---|---|---|---|
| | A244 gp120 | 92TH023 gp120 | MN gp120 | sCD4 binding to A244 gp120 | sCD4 binding to JRFL gp120 | b12 binding to JRFL gp120 |
| T141485 | | | | | | |
| CH20 | − | ++ | ++ | − | − | − |
| T141449 | | | | | | |
| CH77 | ++ | +++ | +++ | 22 | − | − |
| CH89 | + | ++ | ++ | − | − | − |
| CH92 | − | − | ++ | − | − | − |
| CH80 | + | − | ++ | 23 | − | 26 |
| CH29 | − | − | +++ | − | − | − |
| CH78 | ++ | +++ | ++ | 27 | 36 | 29 |
| CH94 | +++ | +++ | +++ | − | − | − |
| CH90 | − | − | +++ | − | − | − |
| CH91 | ++ | +++ | +++ | − | − | − |
| T143859 | | | | | | |
| CH23 | +++ | +++ | +++ | 36 | − | − |
| 609107 | | | | | | |
| CH81 | − | − | +++ | − | − | − |
| CH40 | +++ | ++ | +++ | 46 | 20 | 25 |
| 210884 | | | | | | |
| CH49 | +++ | − | − | − | − | − |
| CH53 | +++ | +++ | +++ | − | − | − |
| CH52 | +++ | +++ | +++ | 32 | − | 30 |
| CH55 | + | − | ++ | 31 | − | 40 |
| CH54 | + | − | +++ | − | − | − |
| CH51 | ++ | − | +++ | − | − | − |
| 347759 | | | | | | |
| CH57 | − | +++ | +++ | − | − | − |
| CH38 | ++ | +++ | +++ | − | − | − |
| Controls | | | | | | |
| A32 | | | | 29 | − | 23 |
| Palivizumab | | | | − | − | − |
| VRC-CH31 | | | | 97 | 67 | 70 |

[a] PTID, participant identity.
[b] +++, 50% inhibitory concentration ($IC_{50}$) of <10 nM; ++, $IC_{50}$ between 10 and 100 nM; +, $IC_{50}$ between 0.1 and 1 μM; −, negative/no binding/no blocking.

The frequency of VH1 gene usage among vaccine-induced HIV-specific ADCC-mediating antibodies also was higher than those of other published data sets: in HIV-1-negative subjects, Brezinschek and colleagues reported the frequency of VH1 genes to be approximately 13% (9/71 reported in reference 6; $P < 0.0001$ by Fisher's exact test comparing the ADCC-mediating antibodies), while in chronically HIV-1-infected subjects the frequency of VH1 usage in anti-HIV-1 antibodies was reported to be 39% (76/193 reported in reference 5; $P = 0.003$ by Fisher's exact test comparing the ADCC-mediating antibodies). We have recently reported frequencies of HIV-1 reactive antibodies using VH1 gene segments of 16.4% (11/67) in HIV-1 acutely infected subjects, which is similar to VH1 usage reported in the National Center for Biotechnology Information database (15.2%; 5,238/34,384) (24), and 38.2% (13/34) in vaccine recipients enrolled in an unrelated HIV-1 vaccine trial (29). In both cases, the frequency of VH1 gene segment usage in ALVAC-HIV/AIDSVAX B/E-induced ADCC-mediating antibodies was significantly higher ($P < 0.0001$ and $P = 0.014$, respectively, by Fisher's exact test). In the present study, none of the recovered ADCC antibodies were clonally related, and VH1 antibodies were recovered from 5/6 vaccinees studied. Thus, the high frequency of usage of VH1 heavy-chain genes among antibodies that mediate ADCC suggests that B cells using those genes have been preferentially selected by the vaccine trial Env proteins.

It is possible that this phenomenon relates to properties of gp120 more generally. Analysis of a different HIV-1 vaccine trial resulted in the recovery of 13/34 (38%) MAbs that used VH1 genes, including 2 MAbs with ADCC activity and 1 with neutralizing activity (29). In contrast, only 12/252 (5%) influenza virus-specific antibodies recovered after influenza immunization (30) used VH1 genes.

**ADCC activity of antibodies using VH1 genes correlated with the degree of somatic mutation.** A number of recent studies have suggested that highly somatically mutated anti-CD4bs bNAbs preferentially use the VH1 gene, in particular the VH 1-2*02 and 1-46 segments, and common amino acid sequence

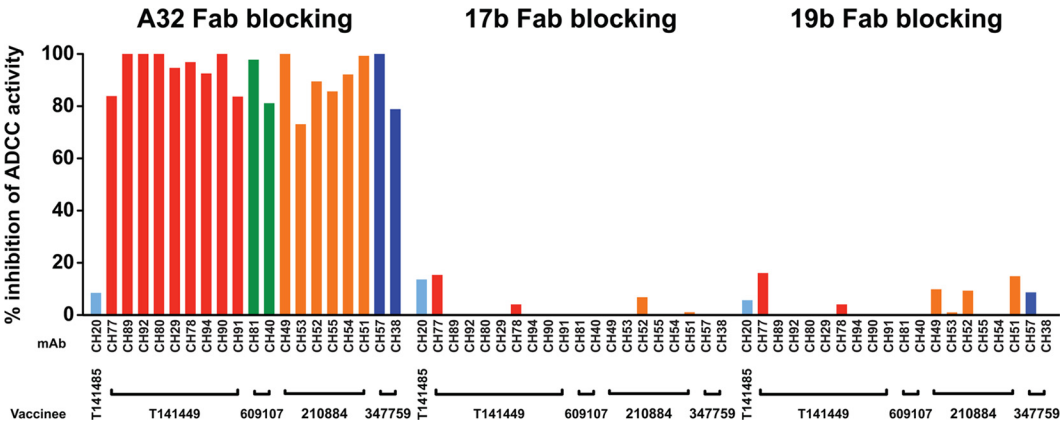


**FIG 4** Monoclonal antibody competition of A32, 17B, and 19B Fab ADCC activity. The 20 ADCC-mediating MAbs that did not bind to linear epitopes were tested for their ability to inhibit ADCC mediated by Fab A32 (left), 17B (middle), and 19B (right) in the ADCC-E.CM235 assay. The *y* axis shows the average inhibition of ADCC activity in duplicate assays, and each bar is color-coded by subject as described for Fig. 3.

motifs (HAAD motifs) have been described for both the heavy and light chains of such anti-CD4bs bNAbs (41, 51). It was striking that among the ADCC-mediating VH1 antibodies that we recovered, 10/17 (59%) used the VH1-2*02 gene segment (Fig. 7). None of the MAbs recovered from this group of participants had broad neutralizing activity, and of the MAbs reported here, only the V3-specific MAb CH23 (VH3-66) displayed tier 1 strain-specific neutralizing activity (28). We sought to determine if this group of antibodies shared the previously described HAAD motifs with the potent CD4bs bNAbs (41). Alignments of the amino acid sequences of the 17 vaccine-induced ADCC-mediating antibodies that used VH1 with the heavy- and light-chain HAAD consensus motifs showed a high degree of similarity (range, 46 to 57 matching amino acids [aa] of 68 aa for the heavy chain, 68 to 84%, and 37 to 46 matching aa of 53 aa for the light chain, 70 to 87%) (Fig. 8A, red circles), which was comparable to the levels of similarity of the CD4bs bNAbs (Fig, 8A, black crosses). We also analyzed a group of three non-HIV-1-reactive VH1-2 anti-influenza virus antibodies that mediate broad influenza virus neutralization (49), which showed a similar degree of heavy-chain homology (52 to 55 matching aa, 76 to 81%) but less homology for the light chain (31 to 32 matching aa, 58 to 60%) (Fig. 8A, blue diamonds). Thus, the similarity of the RV144 vaccine-induced antibodies to the HAAD motif may not reflect functional selection but rather similarities in Env selection of B cells with similar heavy- and light-chain pairings.

Since the broadly neutralizing CD4bs antibodies are also highly mutated, we sought to determine if the degree of somatic mutation in the RV144-induced antibodies correlated with function. We found that the ability to block sCD4 binding did not correlate with the degree of somatic mutation (Fig. 8B). In contrast, the overall strength of ADCC activity, as measured by maximal percent GzB activity against CM235-infected $CD4^+$ T cells, did correlate with heavy-chain somatic mutation (Spearman correlation, $\rho = 0.56$; $P = 0.02$) (Fig. 8B).

## DISCUSSION

The induction of neutralizing antibody (NAb) and cytotoxic T-lymphocyte (CTL) responses are key goals for HIV-1 vaccine de-

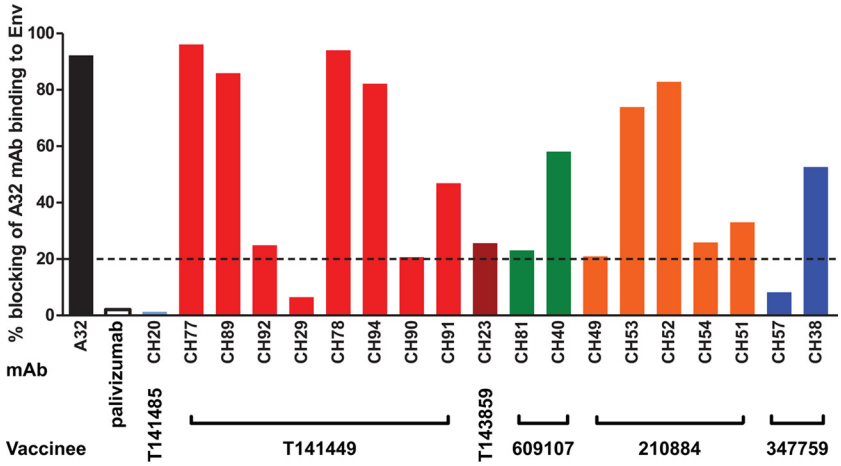


**FIG 5** Monoclonal antibody competition of A32 MAb binding to HIV-1 AE.A244 gp120 envelope glycoprotein. The ADCC-mediating MAbs (with the exception of CH55 and CH80) were tested for their ability to compete for MAb A32 binding to AE.A244 gp120 envelope glycoprotein. The *y* axis shows the percentage of blocking of binding activity, and each bar is color-coded by subject as described for Fig. 3. The data shown are representative of duplicate independent experiments.

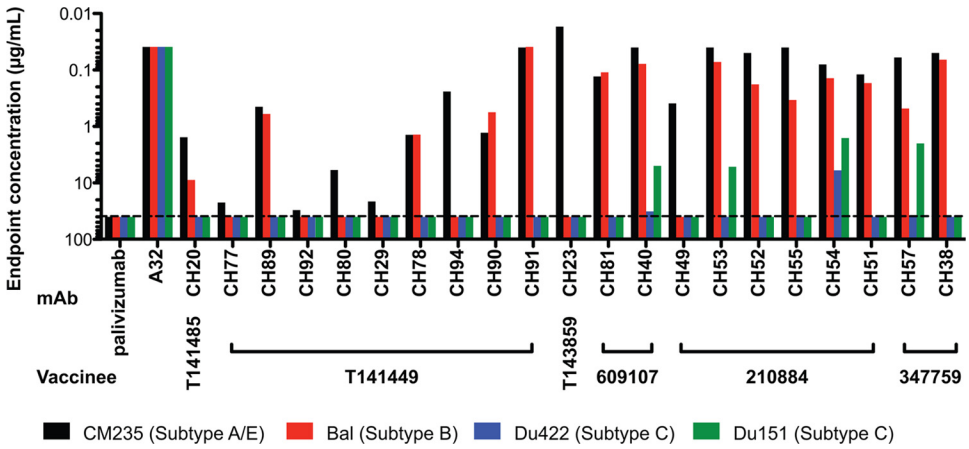


**FIG 6** Cross-clade activity of RV144-induced, ADCC-mediating MAbs. Twenty-one MAbs isolated from six vaccine recipients were tested against CEM.NKR$_{CCR5}$ target cells infected with E.CM235 (black bar), B.BaL (red bar), C.DU422 (blue bar), and C.DU151 (green bar) using the GTL assay. The plot shows the average endpoint titer from duplicate values expressed in μg/ml for each MAb and calculated as previously described for Fig. 3.

velopment. Recently, the phase III efficacy trial of the prime-boost combination of vaccines containing ALVAC-HIV and AIDSVAX B/E has offered the first evidence of vaccine-induced partial protection in humans (39). The vaccine appeared to induce NAb responses with a narrow specificity profile and minimal CD8$^+$ CTL responses (39), suggesting that nonneutralizing Ab and cellular responses other than those of CD8$^+$ CTL have played a role in conferring protection.

A number of studies have suggested that ADCC play an important role in the control of SIV and HIV-1 infection. Several studies have shown that the magnitude of ADCC Ab responses correlates inversely with virus set point in acute SIV infection in both unvaccinated macaques (45) and in vaccinated animals after challenge (2, 7, 14, 15). In humans, ADCC-mediating Abs have been shown to protect against HIV-1 infection in mother-to-infant transmission (26, 33) and to correlate with both control of virus replication (22) and lack of progression to overt disease (3). In contrast, weakly neutralizing and nonneutralizing antibodies were shown to not protect against vaginal simian-human immunodeficiency virus (SHIV) challenge in macaques (8).

ADCC is one of the mechanisms that might have conferred protection from infection in RV144 (17). For this reason, we sought to isolate MAbs that can mediate ADCC from ALVAC-HIV/AIDSVAX B/E vaccine recipients and determine their specificity, clonality, and maturation. In this study, we have demonstrated that the ALVAC-HIV/AIDSVAX B/E vaccine elicited antibodies that mediate ADCC in the majority of the vaccinated subjects, which is in line with previous observations (17, 21), and that gp120 C1 region-specific A32-like antibodies significantly contributed to the overall ADCC responses. By isolating 23 ADCC-mediating MAbs from multiple vaccine recipients, we also demonstrated the presence of ADCC-mediating MAbs of additional specificities. In addition, we determined that the ADCC-mediating MAbs underwent limited affinity maturation and preferentially used VH1 gene segments.

Antibody responses that mediate ADCC were directed toward A32-blockable conformational epitopes ($n = 19$), a non-A32-blockable conformational epitope ($n = 1$), the gp120 Env V2 region ($n = 2$) (23), and a linear epitope in the gp120 V3 region ($n = 1$). The conformational epitope recognized by the A32 MAb is a dominant target of HIV-1-positive plasma ADCC antibodies (13), and A32-like MAbs are among the anti-HIV-1 CD4i Ab responses that are detected following HIV-1 transmission (38, 40). The identification of A32-like MAbs in vaccine recipients suggests that the gp120 epitope recognized by the A32 MAb is an immunodominant region not just in response to natural infection but also upon vaccination. Our data suggest that this A32-binding region reacts with antibodies that have a diverse binding profile, suggesting that the RV144 vaccine targeted multiple related but distinct conformational epitopes on gp120. These epitopes have been shown to be upregulated on the RV144 immunogen and to be efficiently presented by novel Env designs (S. M. Alam, unpublished data), thus it will be possible to test this vaccine strategy in future vaccine trials targeted to different HIV-1 subtypes.

In contrast to ADCC-mediating antibodies, HIV-1 bNAb responses have been reported to appear an average of 2 to 4 years after HIV-1 transmission (16, 27, 42), suggesting that different levels of Ab

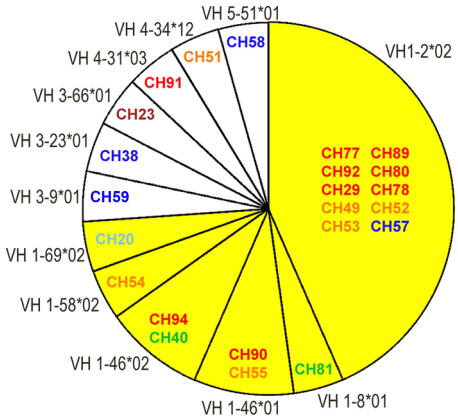


**FIG 7** VH gene segment usage of the ADCC-mediating monoclonal antibodies. The pie chart shows the distribution of VH gene segments and allele usage of the 23 ADCC-mediating MAbs. Each antibody is color-coded by subject of origin using the same color scheme as that described for Fig. 3. The yellow fill indicates all MAbs that used VH1.

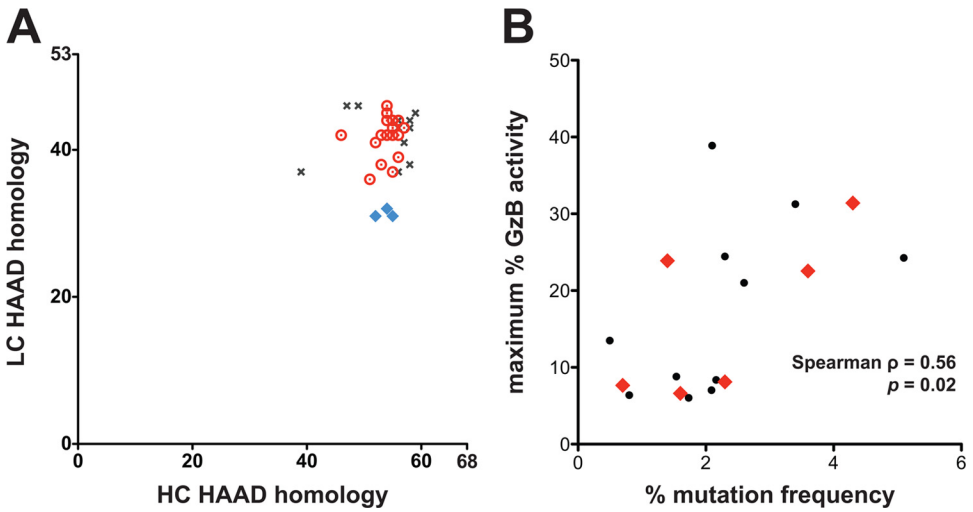


**FIG 8** Characteristics of antibodies that used VH1 gene segments. (A) Amino acid sequences of ADCC-mediating antibodies that used VH1 gene segments were aligned to the heavy- and light-chain consensus HAAD motifs previously identified for CD4bs bNAbs, which were described to preferentially use the VH1 gene, in particular the VH 1-2*02 and 1-46 segments (41). The consensus HAAD motifs of the heavy and light chains are 68 and 53 amino acids long, respectively. Data are plotted as the number of identical amino acids for heavy chain (*x* axis) and light chain (*y* axis). Black X, CD4bs bNAbs (41); red circles, VH1 ADCC mediating antibodies (range, 46- to 57/68-aa identity for heavy chain, 68 to 84%, and 37- to 46/53-aa identity for light chain, 70 to 87%); blue diamonds, influenza virus broadly neutralizing antibodies (49) (52- to 55/68-aa identity for heavy chain, 76 to 81%, and 31- to 32/53-aa identity for light chain, 58 to 60%). (B) Maximal percent GzB activity is correlated with HC mutation frequency (Spearman correlation, $\rho = 0.56$; $P = 0.02$). Antibodies that blocked sCD4 binding to gp120 are shown as red diamonds and were found throughout the range of mutation frequencies; those without blocking activity are shown as black circles.

maturation are required to mediate ADCC and neutralizing activities. Indeed, the mutation frequencies observed in the MAbs isolated from the ALVAC-HIV/AIDSVAX B/E vaccine recipients in our study were low (0.5 to 5.1%) and well below the ~6% changes in variable-domain amino acid sequences commonly seen as greater affinity for the cognate antigen is acquired (30, 50). We did, however, find that higher degrees of VH somatic mutation correlated with greater maximal percent GzB activity (Fig. 8B), consistent with vaccine-driven affinity maturation. Whether repeated boosting of vaccine recipients would result in on-going maturation of these antibodies to further increase ADCC activity, CD4 blocking, or addition of neutralizing activity remains to be determined.

Finally, while ADCC-mediating MAbs were isolated that used diverse VH genes, we observed a clear preferential usage of the VH1 heavy-chain gene (74%) similar to that of potent bNAbs directed against the CD4bs (41, 52). Therefore, while these findings prove that the ADCC-mediating response in these subjects was not restricted to a specific VH gene family and are consistent with there being no obvious strong regulatory mechanisms that would inherently limit the generation of antibodies with ADCC activity, the preferential use of the VH1 gene raises the possibility that the Env proteins used in RV144 or Env gp120 proteins in general preferentially induce the use of the VH1 gene family. Whether a vaccine regimen can be developed that will harness the observed Ig VH1 gene-using B cells to also induce CD4bs antibodies with a high degree of mutation is currently unknown. It is interesting that we were able to recover ADCC antibodies with a degree of CD4 blocking activity that had low levels of mutation, suggesting that B cells expressing those antibodies can be harnessed to produce the desired potent CD4-blocking antibody response under the right conditions.

In summary, the ALVAC-HIV/AIDSVAX B/E vaccine induced potent ADCC responses mediated by modestly mutated and predominantly A32-blockable MAbs that have overlapping but distinct binding profiles. This response is qualitatively similar to anti-HIV-1 responses observed during chronic HIV-1 infections and may have been partly responsible for the modest degree of protection observed. ADCC-mediating MAbs predominantly utilized the VH1 Ig heavy-chain family, which has been previously reported for CD4bs-directed broadly neutralizing antibodies. This observation raises the possibility that continued boosting with this vaccine formulation leads to further somatic mutations of VH1 gp120-specific antibodies and, perhaps, to an enhanced ability to augment any protective effect they might have had to limit HIV-1 acquisition.

## ACKNOWLEDGMENTS

We thank Robert J. Parks, Krissey E. Lloyd, Bradley Lockwood, Mark Drinker, Lawrence Armand, Joshua Eudailey, Neil Meguid, Brandy Ward, and Faraha Brewer for excellent technical assistance. We also thank the following members of the Thai AIDS Vaccine Evaluation Group: (i) from AFRIMS, N. Sirisopana, S. Sukwit, S. Tabprasit, A. Kleebmontha, V. Kamonsin, P. Panjapornsuk, S. Akapirat, W. Kaneechit, C. Chuenchitra, P. Chanbancherd, W. Lokpicaht, R. Paris, B. Merrell, J.-L. Excler, S. Wongkamhaeng, A. Triampon, P. Buapunth, S. Chinaworapong, R. Trichavaroj, S. Chantakulkij, N. Khaochalod, S. Mason, P. Srisaengchai, S. Chanthong, Y. Poangngern, and A. Brown; (ii) from the Vaccine Trials Centre, Mahidol University, W. Supamaranond, S. Naksrisuk, W. Peonim, N. Thantamnu, and R. Muanoum; (iii) from Siriraj Hospital, Prasert Thongcharoen; and (iv) from the Research Institute of Health Sciences, Chiang Mai University, Vinai Suriyanon.

The views expressed in this article are those of the authors and do not reflect the official policy of the Department of the Army, Department of Defense, or the U.S. Government.

This work was supported by the National Institutes of Health (NIH), National Institutes of Allergies and Infectious Diseases (NIAID), the Division of AIDS with the Center for HIV/AIDS Vaccine Immunology (CHAVI) (grant U19 AI067854); by a Collaboration for AIDS Vaccine Discovery (CAVD) grant to B.F.H. from the Bill and Melinda Gates Foundation; in part by Interagency Agreement Y1-AI-2642-12 between U.S. Army Medical Research and Materiel Command (USAMRMC) and the NIAID. In addition, this work was supported by a cooperative agreement

(W81XWH-07-2-0067) between the Henry M. Jackson Foundation for the Advancement of Military Medicine, Inc., and the U.S. Department of Defense. Additional support was provided by the CAVD from the Bill and Melinda Gates Foundation (grants 38619 to G.F. and D.C.M. and 38650 to G.F.). J.P. was supported by the NIH, NIAID grant AI07392.

## REFERENCES

1. **Adachi A, et al.** 1986. Production of acquired immunodeficiency syndrome-associated retrovirus in human and nonhuman cells transfected with an infectious molecular clone. J. Virol. **59**:284–291.
2. **Barouch DH, et al.** 2012. Vaccine protection against acquisition of neutralization-resistant SIV challenges in rhesus monkeys. Nature **482**:89–93.
3. **Baum LL, et al.** 1996. HIV-1 gp120-specific antibody-dependent cell-mediated cytotoxicity correlates with rate of disease progression. J. Immunol. **157**:2168–2173.
4. **Bonsignori M, et al.** 2011. Analysis of a clonal lineage of HIV-1 envelope V2/V3 conformational epitope-specific broadly neutralizing antibodies and their inferred unmutated common ancestors. J. Virol. **85**:9998–10009.
5. **Breden F, et al.** 2011. Comparison of antibody repertoires produced by HIV-1 infection, other chronic and acute infections, and systemic autoimmune disease. PLoS One **6**:e16857. doi:10.1371/journal.pone.0016857.
6. **Brezinschek HP, Brezinschek RI, Lipsky PE.** 1995. Analysis of the heavy chain repertoire of human peripheral B cells using single-cell polymerase chain reaction. J. Immunol. **155**:190–202.
7. **Brocca-Cofano E, et al.** 2011. Vaccine-elicited SIV and HIV envelope-specific IgA and IgG memory B cells in rhesus macaque peripheral blood correlate with functional antibody responses and reduced viremia. Vaccine **29**:3310–3319.
8. **Burton DR, et al.** 2011. Limited or no protection by weakly or nonneutralizing antibodies against vaginal SHIV challenge of macaques compared with a strongly neutralizing antibody. Proc. Natl. Acad. Sci. U. S. A. **108**:11181–11186.
9. **DeVico A, et al.** 2007. Antibodies to CD4-induced sites in HIV gp120 correlate with the control of SHIV challenge in macaques vaccinated with subunit immunogens. Proc. Natl. Acad. Sci. U. S. A. **104**:17477–17482.
10. **Edmonds TG, et al.** 2010. Replication competent molecular clones of HIV-1 expressing Renilla luciferase facilitate the analysis of antibody inhibition in PBMC. Virology **408**:1–13.
11. **Ewing B, Green P.** 1998. Base-calling of automated sequencer traces using phred. II. Error probabilities. Genome Res. **8**:186–194.
12. **Ewing B, Hillier L, Wendl MC, Green P.** 1998. Base-calling of automated sequencer traces using phred. I. Accuracy assessment. Genome Res. **8**:175–185.
13. **Ferrari G, et al.** 2011. A HIV-1 gp120 envelope human monoclonal antibody that recognizes a C1 conformational epitope mediates potent ADCC activity and defines a common ADCC epitope in human HIV-1 serum. J. Virol. **85**:7029–7036.
14. **Florese RH, et al.** 2009. Contribution of nonneutralizing vaccine-elicited antibody activities to improved protective efficacy in rhesus macaques immunized with Tat/Env compared with multigenic vaccines. J. Immunol. **182**:3718–3727.
15. **Gómez-Román VR, et al.** 2005. Vaccine-elicited antibodies mediate antibody-dependent cellular cytotoxicity correlated with significantly reduced acute viremia in rhesus macaques challenged with SIVmac251. J. Immunol. **174**:2185–2189.
16. **Gray ES, et al.** 2011. Isolation of a monoclonal antibody targeting the alpha-2 helix of gp120 representing the initial autologous neutralizing antibody response in an HIV-1 subtype C infected individual. J. Virol. **85**:7719–7729.
17. **Haynes BF, et al.** 2012. Immune-correlates analysis of an HIV-1 vaccine efficacy trial. N. Engl. J. Med. **366**:1275–1286.
18. **Hidajat R, et al.** 2009. Correlation of vaccine-elicited systemic and mucosal nonneutralizing antibody activities with reduced acute viremia following intrarectal simian immunodeficiency virus SIVmac251 challenge of rhesus macaques. J. Virol. **83**:791–801.
19. **Johnson S, et al.** 1997. Development of a humanized monoclonal antibody (MEDI-493) with potent in vitro and in vivo activity against respiratory syncytial virus. J. Infect. Dis. **176**:1215–1224.
20. **Kabat EA, Wu TT, Perry MH, Gottesman KS, Foeller C.** 1991. Sequences of proteins of immunological interest, 5th ed. U.S. Department of Health and Human Services, Bethesda, MD.
21. **Karnasuta C, et al.** 2005. Antibody-dependent cell-mediated cytotoxic responses in participants enrolled in a phase I/II ALVAC-HIV/AIDSVAX B/E prime-boost HIV-1 vaccine trial in Thailand. Vaccine **23**:2522–2529.
22. **Lambotte O, et al.** 2009. Heterogeneous neutralizing antibody and antibody-dependent cell cytotoxicity responses in HIV-1 elite controllers. AIDS **23**:897–906.
23. **Liao HX, et al.** 2012. HIV-1 envelope antibodies induced by ALVAC-AIDSVAX B/E vaccine target a site of vaccine immune pressure within the C β-strand of gp120 V1/V2, abstr 230, p 110. Keystone Symp. HIV Vaccines.
24. **Liao HX, et al.** 2011. Initial antibodies binding to HIV-1 gp41 in acutely infected subjects are polyreactive and highly mutated. J. Exp. Med. **208**:2237–2249.
25. **Liao HX, et al.** 2009. High-throughput isolation of immunoglobulin genes from single human B cells and expression as monoclonal antibodies. J. Virol. Methods **158**:171–179.
26. **Ljunggren K, et al.** 1990. Antibodies mediating cellular cytotoxicity and neutralization correlate with a better clinical stage in children born to human immunodeficiency virus-infected mothers. J. Infect. Dis. **161**:198–202.
27. **Mikell I, et al.** 2011. Characteristics of the earliest cross-neutralizing antibody response to HIV-1. PLoS Pathog. **7**:e1001251. doi:10.1371/journal.ppat.1001251.
28. **Montefiori DC, et al.** Magnitude and breadth of the neutralizing antibody response in the RV144 and Vax003 HIV-1 vaccine efficacy trials. J. Infect. Dis. **206**:431–441.
29. **Moody MA, et al.** 2012. HIV-1 gp120 vaccine induces affinity maturation in both new and persistent antibody clonal lineages. J. Virol. **86**:7496–7507.
30. **Moody MA, et al.** 2011. H3N2 influenza infection elicits more cross-reactive and less clonally expanded anti-hemagglutinin antibodies than influenza vaccination. PLoS One **6**:e25797. doi:10.1371/journal.pone.0025797.
31. **Moore JP, et al.** 1995. A human monoclonal antibody to a complex epitope in the V3 region of gp120 of human immunodeficiency virus type 1 has broad reactivity within and outside clade B. J. Virol. **69**:122–130.
32. **Munshaw S, Kepler TB.** 2010. SoDA2: a Hidden Markov Model approach for identification of immunoglobulin rearrangements. Bioinformatics **26**:867–872.
33. **Nag P, et al.** 2004. Women with cervicovaginal antibody-dependent cell-mediated cytotoxicity have lower genital HIV-1 RNA loads. J. Infect. Dis. **190**:1970–1978.
34. **Nitayaphan S, et al.** 2004. Safety and immunogenicity of an HIV subtype B and E prime-boost vaccine combination in HIV-negative Thai adults. J. Infect. Dis. **190**:702–706.
35. **O'Doherty U, Swiggard WJ, Malim MH.** 2000. Human immunodeficiency virus type 1 spinoculation enhances infection through virus binding. J. Virol. **74**:10074–10080.
36. **Pollara J, et al.** 2011. High-throughput quantitative analysis of HIV-1 and SIV-specific ADCC-mediating antibody responses. Cytometry A **79**:603–612.
37. **Pollara J, et al.** 2010. Early appearance of ADCC- and ADCVI-mediating antibody responses against autologous HIV-1 transmitted/founder virus. AIDS Res. Hum. Retrovir. **26**:A-12.
38. **Pollara J, et al.** 2011. Ontogeny, breadth and specificity of circulating ADCC-mediating antibodies in HIV-1 infected individuals. AIDS Res. Hum. Retroviruses **27**:A-66.
39. **Rerks-Ngarm S, et al.** 2009. Vaccination with ALVAC and AIDSVAX to prevent HIV-1 infection in Thailand. N. Engl. J. Med. **361**:2209–2220.
40. **Robinson JE, Elliott DH, Martin EA, Micken K, Rosenberg ES.** 2005. High frequencies of antibody responses to CD4 induced epitopes in HIV infected patients started on HAART during acute infection. Hum. Antibodies **14**:115–121.
41. **Scheid JF, et al.** 2011. Sequence and structural convergence of broad and potent HIV antibodies that mimic CD4 binding. Science **333**:1633–1637.
42. **Shen X, et al.** 2009. In vivo gp41 antibodies targeting the 2F5 monoclonal antibody epitope mediate human immunodeficiency virus type 1 neutralization breadth. J. Virol. **83**:3617–3625.
43. **Shields RL, et al.** 2001. High resolution mapping of the binding site on human IgG1 for Fc gamma RI, Fc gamma RII, Fc gamma RIII, and FcRn and design of IgG1 variants with improved binding to the Fc gamma R. J. Biol. Chem. **276**:6591–6604.

44. **Smith TF, Waterman MS.** 1981. Identification of common molecular subsequences. J. Mol. Biol. **147**:195–197.
45. **Sun Y, et al.** 2011. Antibody-dependent cell-mediated cytotoxicity in simian immunodeficiency virus-infected rhesus monkeys. J. Virol. **85**: 6906–6912.
46. **Thali M, et al.** 1993. Characterization of conserved human immunodeficiency virus type 1 gp120 neutralization epitopes exposed upon gp120-CD4 binding. J. Virol. **67**:3978–3988.
47. **Trkola A, Matthews J, Gordon C, Ketas T, Moore JP.** 1999. A cell line-based neutralization assay for primary human immunodeficiency virus type 1 isolates that use either the CCR5 or the CXCR4 coreceptor. J. Virol. **73**:8966–8974.
48. **Volpe JM, Cowell LG, Kepler TB.** 2006. SoDA: implementation of a 3D alignment algorithm for inference of antigen receptor recombinations. Bioinformatics **22**:438–444.
49. **Whittle JR, et al.** 2011. Broadly neutralizing human antibody that recognizes the receptor-binding pocket of influenza virus hemagglutinin. Proc. Natl. Acad. Sci. U. S. A. **108**:14216–14221.
50. **Wrammert J, et al.** 2008. Rapid cloning of high-affinity human monoclonal antibodies against influenza virus. Nature **453**:667–671.
51. **Wu X, et al.** 2010. Rational design of envelope identifies broadly neutralizing human monoclonal antibodies to HIV-1. Science **329**:856–861.
52. **Wu X, et al.** 2011. Focused evolution of HIV-1 neutralizing antibodies revealed by structures and deep sequencing. Science **333**:1593–1602.
53. **Wyatt R, et al.** 1995. Involvement of the V1/V2 variable loop structure in the exposure of human immunodeficiency virus type 1 gp120 epitopes induced by receptor binding. J. Virol. **69**:5723–5733.
54. **Yagita M, et al.** 2000. A novel natural killer cell line (KHYG-1) from a patient with aggressive natural killer cell leukemia carrying a p53 point mutation. Leukemia **14**:922–930.